Supporting Information

The Mechanism of Single-Walled Carbon Nanotube Growth and Chirality Selection Induced by Carbon Atom and Dimer Addition

Qian Wang[†,‡], Man-Fai Ng[‡], Shuo-Wang Yang[‡], Yanhui Yang[†], Yuan Chen[†*]*

†School of Chemical and Biomedical Engineering, Nanyang Technological University, 62 Nanyang Drive, Singapore 637459, Singapore

‡ Institute of High Performance Computing, 1 Fusionopolis Way, #16-16 Connexis, Singapore 138632, Singapore

E-mail: chenyuan@ntu.edu.sg; yangsw@ihpc.a-star.edu.sg

Figure S1. Schematic potential energy surfaces of singlet and triplet for single C atom induced chirality change reactions at the B3LYP/6-31G level.

Figure S2. Schematic potential energy surfaces of singlet (black) and triplet (red) for C_2 dimer addition growth reactions at the B3LYP/6-31G level.

Table S1. The energies of the various caps, intermediates and transition states during the chirality change reaction path at different spin multiplicities.

Table S2. The energies of the various caps, intermediates and transition states during the tube growth reaction path at different spin multiplicities.

Figure S3. Optimized geometries of singlet and triplet intermediates and transition states along the chirality change paths at B3LYP/6-31G level.

Figure S4. Optimized geometries of singlet and triplet intermediates and transition states along the nanotube growth paths at B3LYP/6-31G level.

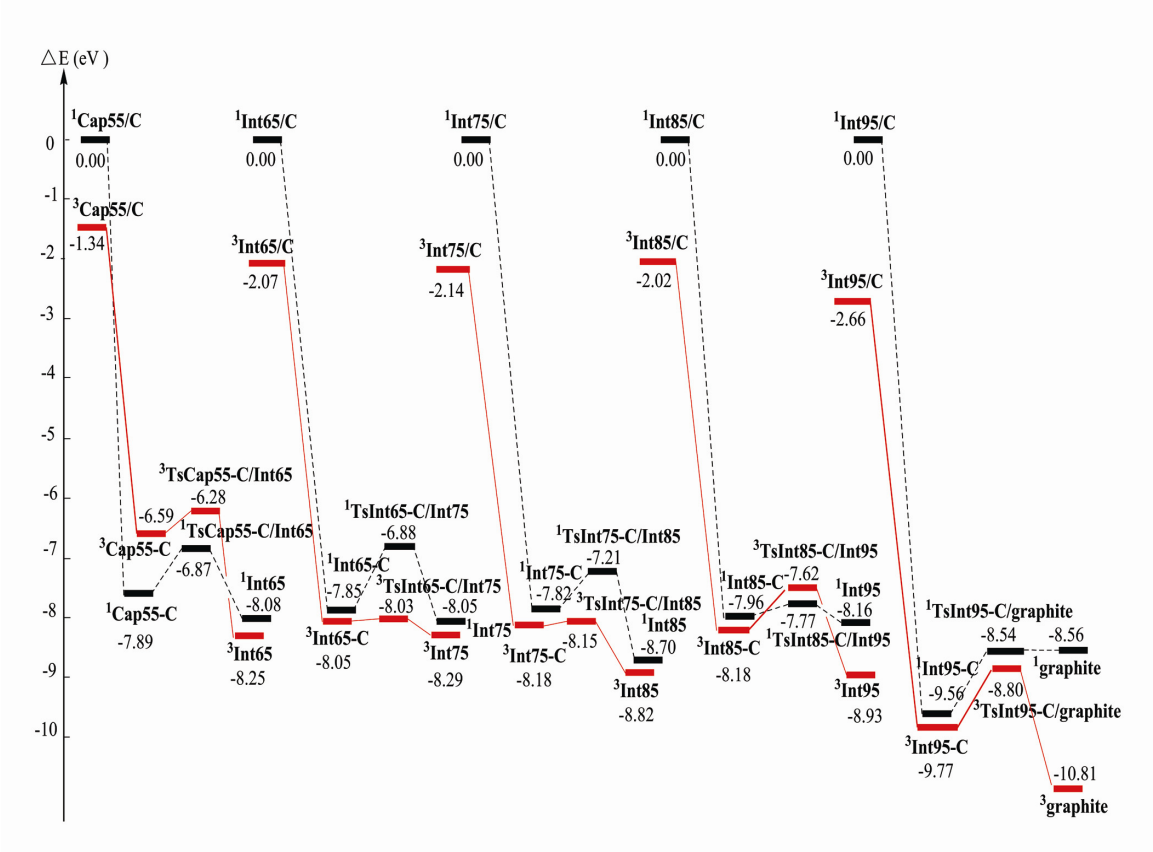

Figure S1. Schematic potential energy surfaces (PESs) of singlet (black) and triplet (red) for single C atom induced chirality change reactions at the B3LYP/6-31G level. The relative energies of ^{1}Cap55/C, ^{1}Cap65/C, ^{1}Cap75/C, ^{1}Cap85/C, and ^{1}Cap95/C are set to zero as references for corresponding species. These singlet and triplet PESs correspond to the blue horizontal arrows in Figure 2, representing the possible chirality change paths induced by individual C atoms. (5,5) armchair cap is chosen as a starting point. The reaction pathways from (5,5) cap to near-armchair (*n*,5) caps (*n* = 6, 7, 8 and 9) are presented. In the throughout discussions in the main text, the term "thermodynamical stability" is referring to the relative energy order. A cap or an intermediate with relatively lower energy is considered to have a higher thermodynamical stability. On the other hand, the kinetic stability is judged by the conversion energy barrier. An intermediate having a lower energy conversion barrier possesses a higher kinetic stability.

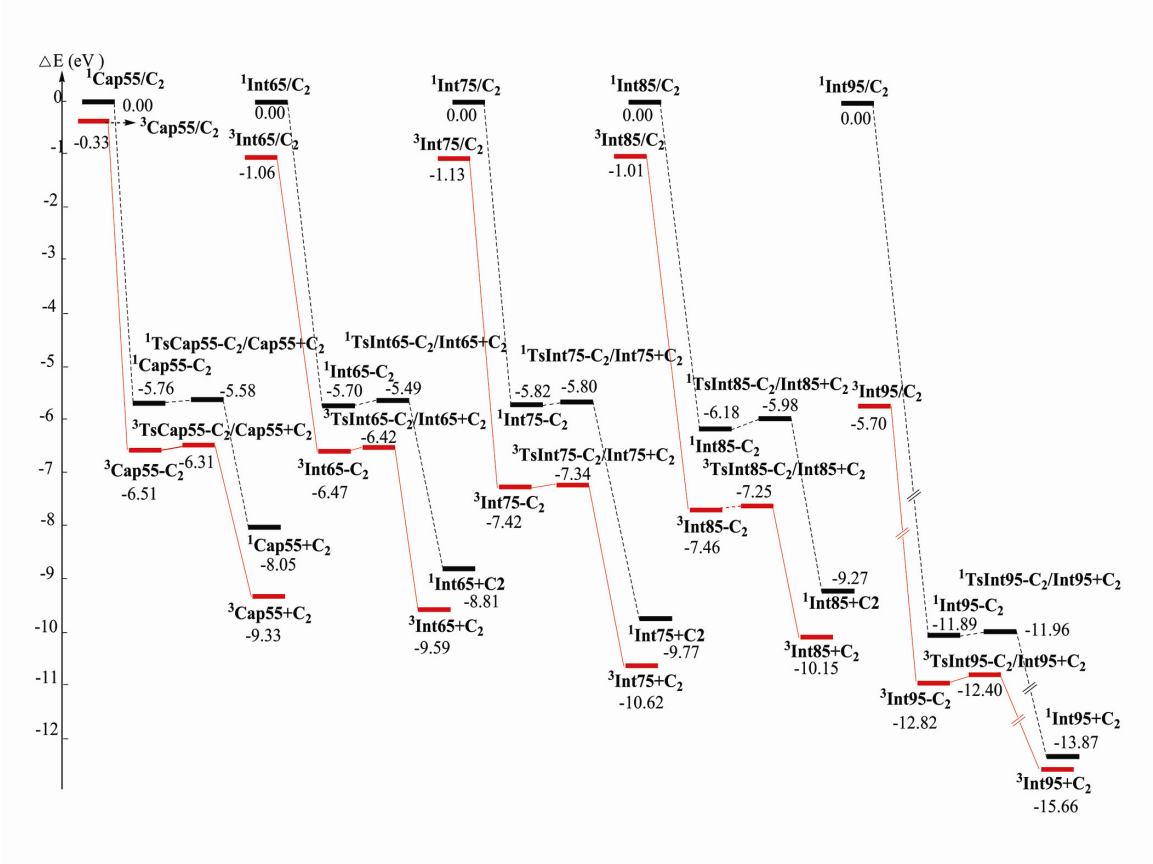

Figure S2. Schematic potential energy surfaces of singlet (black) and triplet (red) for C_2 dimer addition growth reactions at the B3LYP/6-31G level. The relative energies of ^{1}Cap55/C$_2$, ^{1}Int65/C$_2$, ^{1}Int75/C$_2$, ^{1}Int85/C$_2$, and ^{1}Int95/C$_2$ are set to zero as references for corresponding species. These singlet and triplet PESs correspond to the black vertical arrows in Figure 2, representing the cap growth processes leading to corresponding SWCNTs from the specific (n,5) caps (n = 5, 6, 7, 8, and 9).

Table S1: The energies of the various caps, intermediates and transition states during the chirality change reaction path at different spin multiplicities: the total energy (a.u.), zero-point vibrational energy (ZPVE) (kcal/mole), and the relative energies (RE) (in both kcal/mole and eV) (inclusion of the ZPVE). The relative energies of ^{1}Cap55/C, ^{1}Int65/C, ^{1}Int75/C, ^{1}Int85/C and ^{1}Int95/C are set to zero as references for corresponding species.

Species	Total	ZPVE (kcal/mole)	RE (kcal/mol)	RE (eV)
^{1}Cap55/C	-1179.65897	105.37	0.00	0.00
^{1}Cap55-C	-1179.95335	108.23	-181.86	-7.89
^{1}TsCap55-C/Int65	-1179.91250	106.08	-158.38	-6.87
^{1}Int65	-1179.95983	107.94	-186.22	-8.08
^{3}Cap55/C	-1179.70786	105.23	-30.82	-1.34
^{3}Cap55-C	-1179.90376	107.05	-151.92	-6.59
^{3}TsCap55-C/ Int65	-1179.89108	106.16	-144.87	-6.28
^{3}Int65	-1179.96483	107.05	-190.25	-8.25
^{1}Int65/C	-1217.73398	107.94	0.00	0.00
^{1}Int65-C	-1218.02707	110.74	-181.12	-7.85
^{1}TsInt65-C/Int75	-1217.98794	108.72	-158.58	-6.88
^{1}Int75	-1218.03356	110.39	-185.54	-8.05
^{3}Int65/C	-1217.80850	107.05	-47.65	-2.07
^{3}Int65-C	-1218.03368	110.41	-185.60	-8.05
^{3}TsInt65-C/Int75	-1218.02893	107.88	-185.14	-8.03
^{3}Int75	-1218.04124	109.53	-191.22	-8.29
^{1}Int75/C	-1255.80771	110.39	0.00	0.00
^{1}Int75-C	-1256.09934	113.04	-180.35	-7.82
^{1}TsInt75-C/Int85	-1256.07472	111.76	-166.18	-7.21
^{1}Int85	-1256.13449	114.80	-200.65	-8.70
^{3}Int75/C	-1255.88490	109.53	-49.30	-2.14
^{3}Int75-C	-1256.11130	112.29	-188.61	-8.18
^{3}TsInt75-C/Int85	-1256.10939	111.74	-187.95	-8.15
^{3}Int85	-1256.13668	113.32	-203.50	-8.82
^{1}Int85/C	-1293.90865	114.80	0.00	0.00
^{1}Int85-C	-1294.20574	117.60	-183.63	-7.96
^{1}TsInt85-C/Int95	-1294.19679	116.47	-179.14	-7.77
^{1}Int95	-1294.21003	115.83	-188.10	-8.16
^{3}Int85/C	-1293.98035	113.32	-46.47	-2.02
^{3}Int85-C	-1294.21269	116.88	-188.71	-8.18
^{3}TsInt85-C/Int95	-1294.18995	115.60	-175.72	-7.62

^{3}Int95	-1294.23909	116.33	-205.83	-8.93
^{1}Int95/C	-1331.98419	115.83	0.00	0.00
^{1}Int95-C	-1332.33848	122.97	-220.55	-9.56
^{1}TsInt95-C/graphite	-1332.29909	121.04	-196.96	-8.54
^{1}graphite	-1332.30294	118.49	-197.35	-8.56
^{3}Int95/C	-1332.08275	116.33	-61.35	-2.66
^{3}Int95-C	-1332.35350	122.23	-225.35	-9.77
^{3}TsInt95-C/graphite	-1332.31542	120.87	-202.82	-8.80
^{3}graphite	-1332.38732	119.53	-249.26	-10.81
^{1}C	-37.77415			
^{3}C	-37.84366			

Table S2. The energies of the various caps, intermediates and transition states during the tube growth reaction path at different spin multiplicities: the total energy (a.u.), zero-point vibrational energy (ZPVE) (kcal/mole), and the relative energies (RE) (in both kcal/mole and eV) (inclusion of the ZPVE). The relative energy of ^{1}Cap55/C_2, ^{1}Int65/C_2, ^{1}Int75/C_2, ^{1}Int85/C_2 and ^{1}Int95/C_2 are set to zero as references for corresponding species.

Species	Total	ZPVE (kcal/mole)	RE (kcal/mol)	RE (eV)
^{1}Cap55/C_2	-1217.74896	108.02	0.00	0.00
^{1}Cap55-C_2	-1217.96397	110.20	-132.74	-5.76
^{1}TsCap55-C_2/Cap55+C_2	-1217.95713	110.04	-128.61	-5.58
^{1}Cap55+C_2	-1218.05038	111.54	-185.62	-8.05
^{3}Cap55/^{3}C_2	-1217.76045	107.58	-7.65	-0.33
^{3}Cap55-C_2	-1217.99268	110.81	-150.15	-6.51
^{3}TsCap55-C_2/Cap55+C_2	-1217.98514	110.82	-145.41	-6.31
^{3}Cap55+C_2	-1218.10062	113.43	-215.26	-9.33
^{1}Int65/C_2	-1255.82397	110.59	0.00	0.00
^{1}Int65-C_2	-1256.03671	112.60	-131.48	-5.70
^{1}TsInt65-C_2/Int65+C_2	-1256.02857	112.43	-126.55	-5.49
^{1}Int65+C_2	-1256.15666	116.12	-203.23	-8.81
^{3}Int65/^{3}C_2	-1255.86109	109.41	-24.47	-1.06
^{3}Int65-C_2	-1256.06594	113.25	-149.18	-6.47
^{3}TsInt65-C_2/Int65+C_2	-1256.06296	112.47	-148.09	-6.42
^{3}Int65+C_2	-1256.18574	116.50	-221.10	-9.59

^{1}Int75/C_2	-1293.89770	113.04	0.00	0.00
^{1}Int75-C_2	-1294.11481	115.05	-134.23	-5.82
^{1}TsInt75-C_2/Int75+C_2	-1294.11407	115.06	-133.76	-5.80
^{1}Int75+C_2	-1294.26613	118.87	-225.37	-9.77
^{3}Int75/$^3C_2$	-1293.93750	111.88	-26.13	-1.13
^{3}Int75-C_2	-1294.16422	115.82	-164.47	-7.13
^{3}TsInt75-C_2/Int75+C_2	-1294.17231	116.08	-169.28	-7.34
^{3}Int75+C_2	-1294.29891	119.80	-245.00	-10.62
^{1}Int85/C_2	-1331.99864	117.45	0.00	0.00
^{1}Int85-C_2	-1332.23004	120.11	-142.47	-6.18
^{1}TsInt85-C_2/Int85+C_2	-1332.22241	119.88	-137.91	-5.98
^{1}Int85+C_2	-1332.34592	121.43	-213.82	-9.27
^{3}Int85/$^3C_2$	-1332.03294	115.68	-23.28	-1.01
^{3}Int85-C_2	-1332.27697	119.96	-172.05	-7.46
^{3}TsInt85-C_2/Int85+C_2	-1332.26935	119.98	-167.25	-7.25
^{3}Int85+C_2	-1332.37994	122.44	-234.15	-10.15
^{1}Int95/C_2	-1370.07417	211.83	0.00	0.00
^{1}Int95-C_2	-1370.37372	125.51	-274.28	-11.89
^{1}TsInt95-C_2/Int95+C_2	-1370.37596	125.52	-275.69	-11.96
^{1}Int95+C_2	-1370.44458	124.40	-319.86	-13.87
^{3}Int95/$^3C_2$	-1370.13534	118.68	-131.53	-5.70
^{3}Int95-C_2	-1370.40756	125.49	-295.54	-12.82
^{3}TsInt95-C_2/Int95+C_2	-1370.38723	122.31	-285.96	-12.40
^{3}Int95+C_2	-1370.51212	125.57	-361.07	-15.66
$^1C_2$	-75.86414	2.65		
$^3C_2$	-75.89626	2.36		

Figure S3. Optimized geometries of singlet and triplet intermediates at B3LYP/6-31G level. Bond lengths are in angstroms, and angles are in degrees. The structure labels refer to the description in the main text.

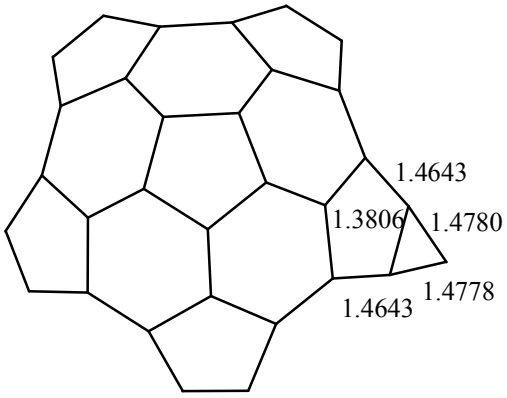

^{1}Cap55-C

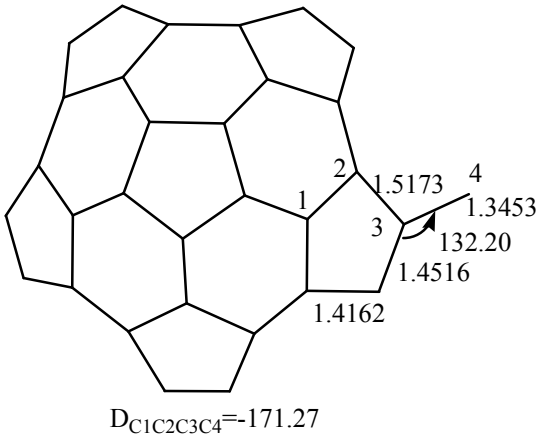

$D_{C1C2C3C4}$=-171.27

^{3}Cap55-C

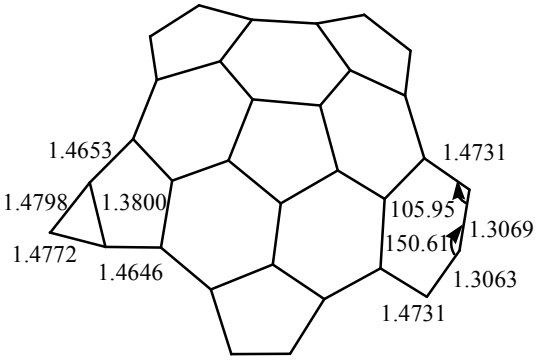

^{1}Int65-C

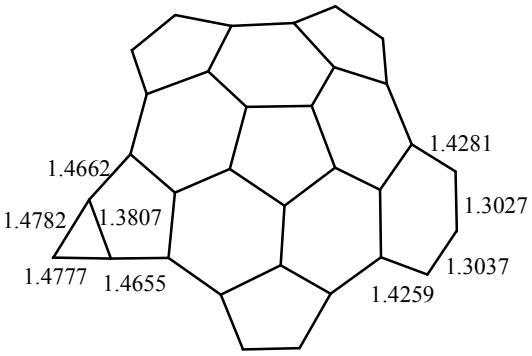

^{3}Int65-C

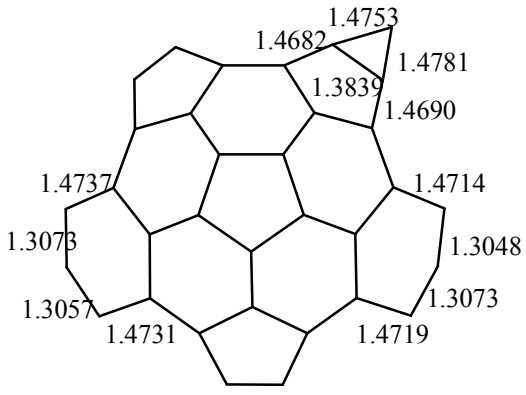

^{1}Int75-C

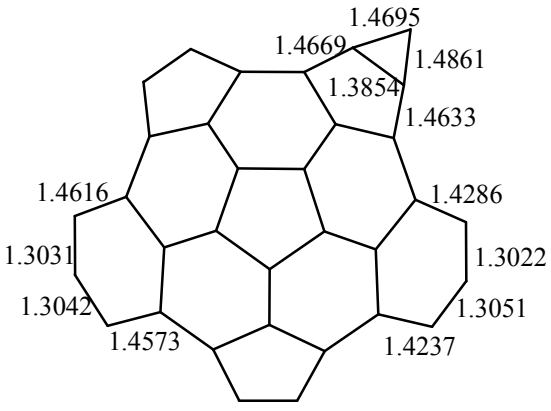

^{3}Int75-C

Figure S3 continued

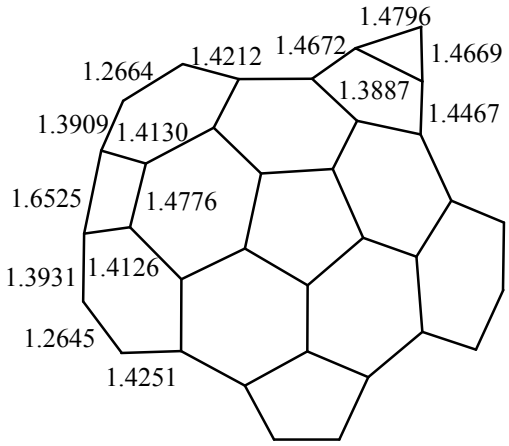

^{1}Int85-C

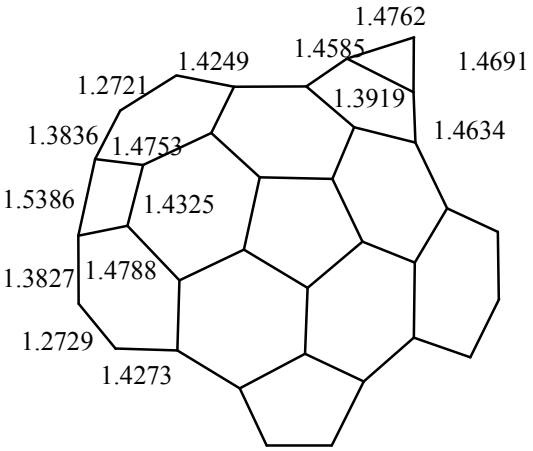

^{3}Int85-C

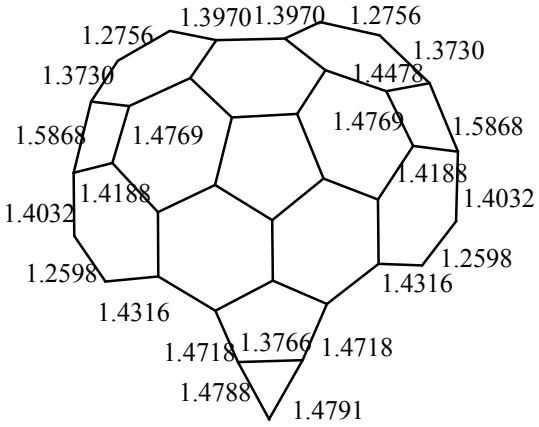

^{1}Int95-C

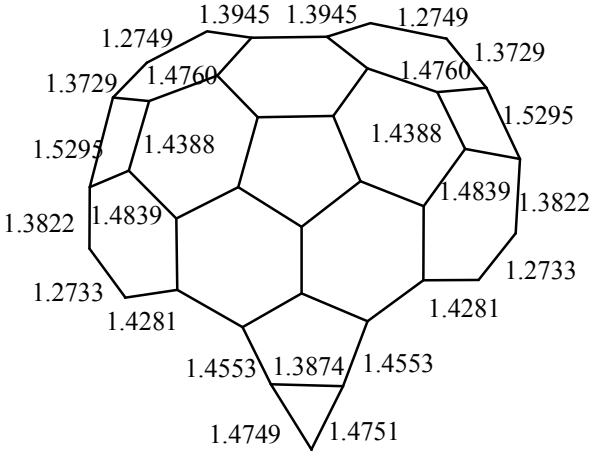

^{3}Int95-C

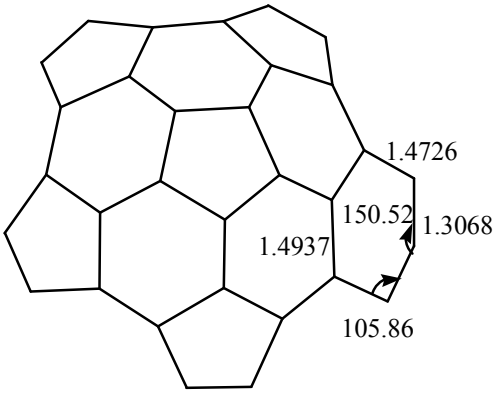

^{1}Int65

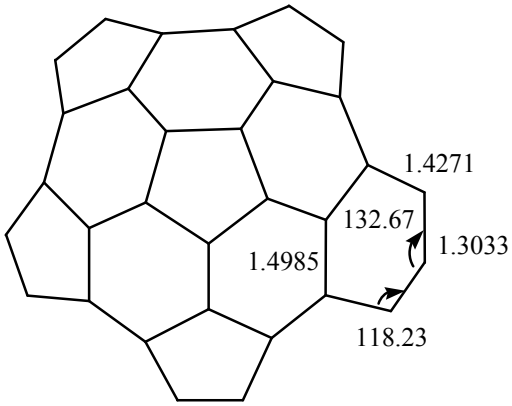

^{3}Int65

Figure S3 continued

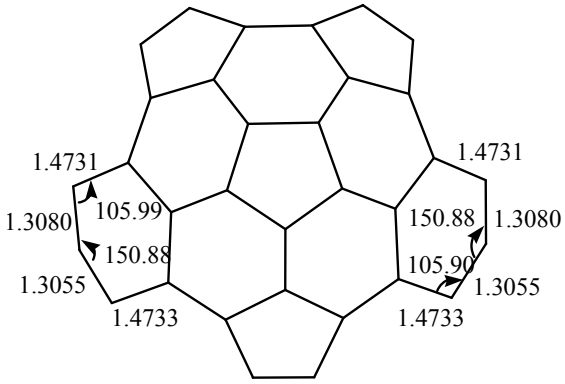

^{1}Int75

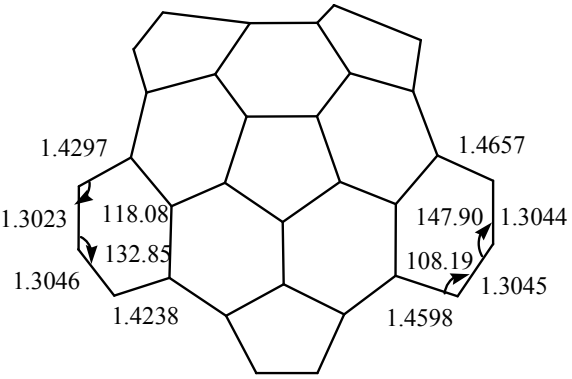

^{3}Int75

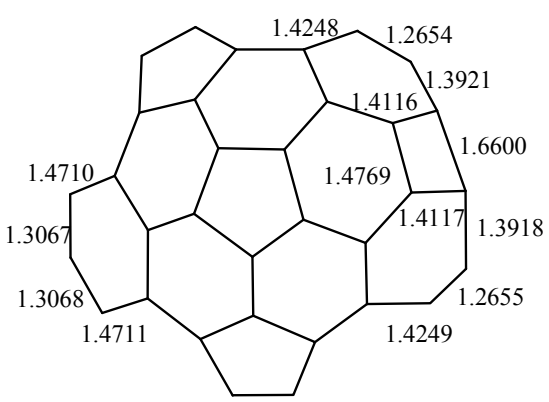

^{1}Int85

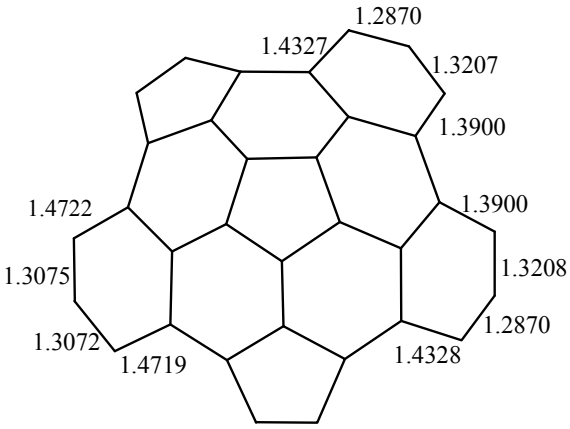

^{3}Int85

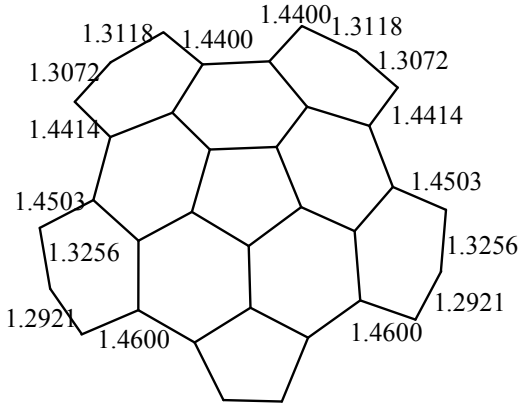

^{1}Int95

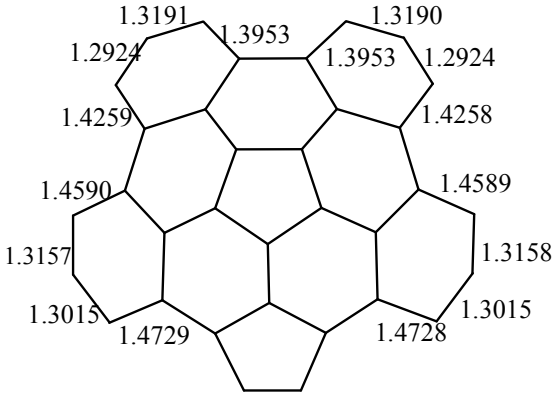

^{3}Int95

Figure S3 continued

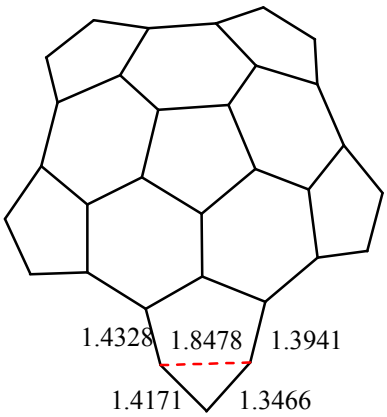

^{1}TsCap55-C/Int65

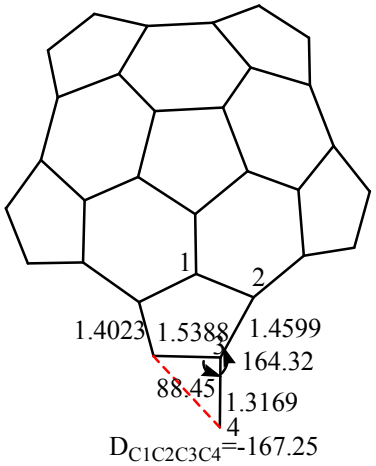

^{3}TsCap55-C/Int65

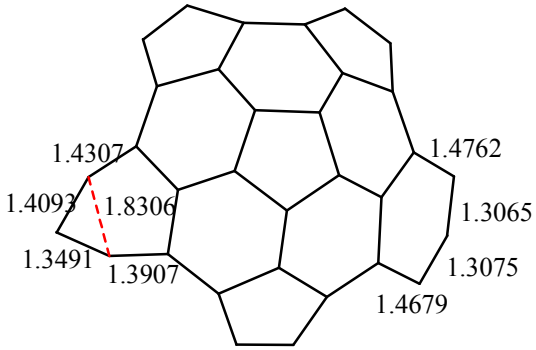

^{1}TsInt65-C/Int75

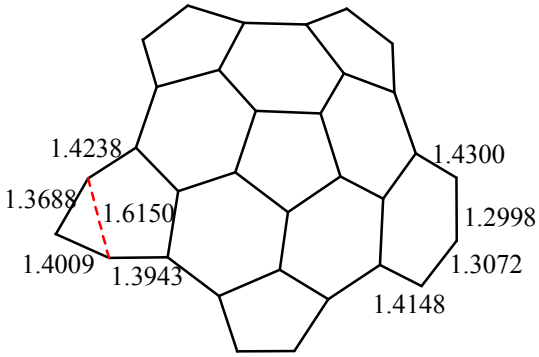

^{3}TsInt65-C/Int75

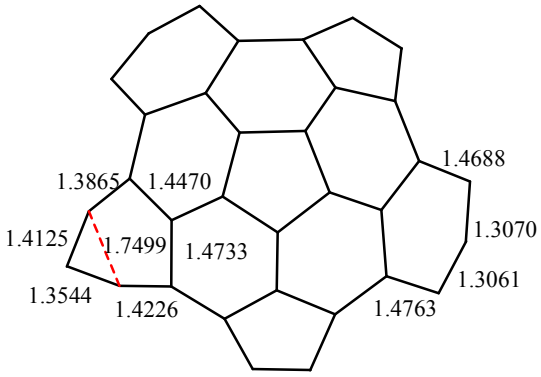

^{1}TsInt75-C/Int85

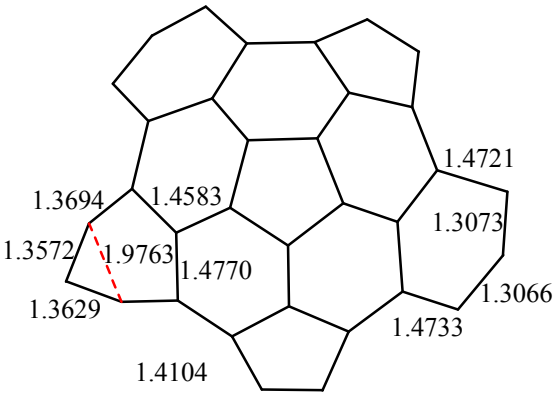

^{3}TsInt75-C/Int85

Figure S3 continued

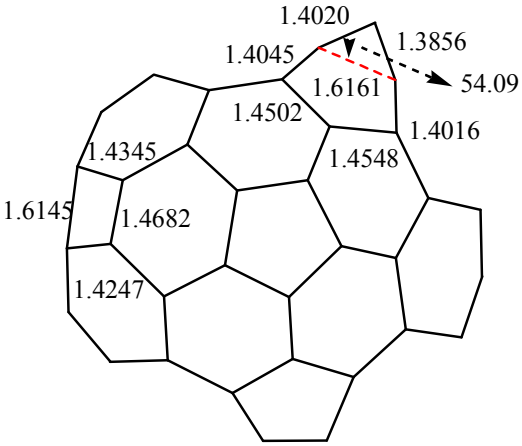

^{1}TsInt85-C/Int95

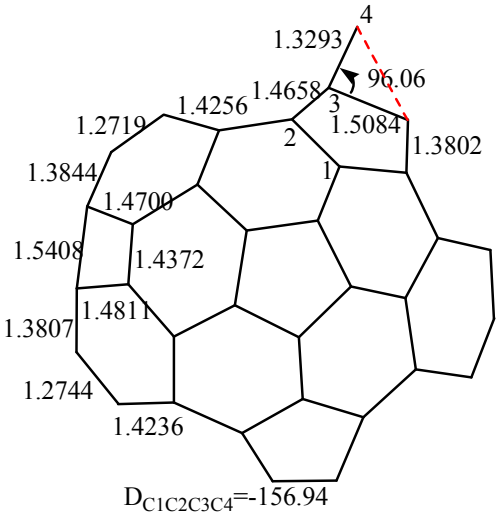

^{3}TsInt85-C/Int95

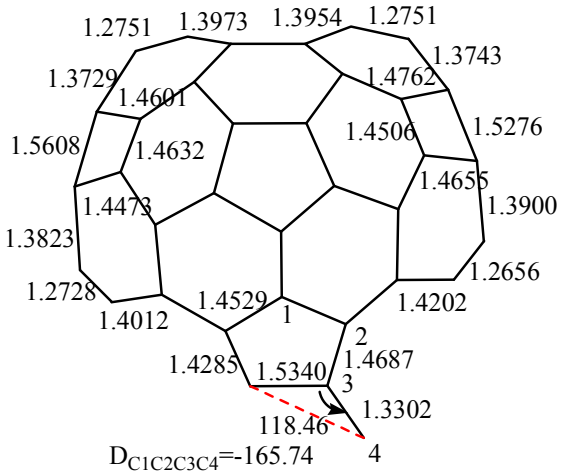

^{1}TsInt95-C/graphite

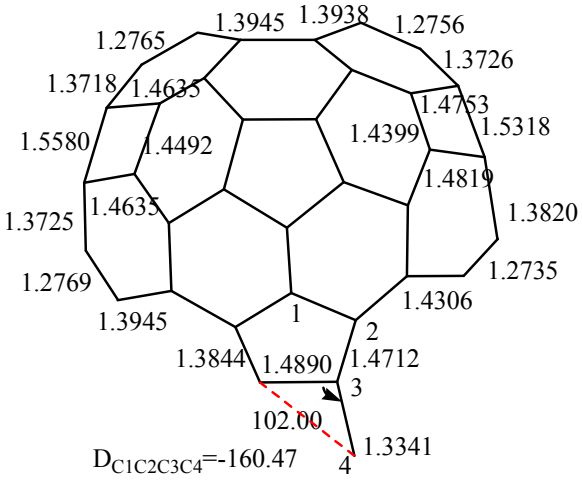

^{3}TsInt95-C/graphite

Figure S4. Optimized geometries of singlet and triplet transition states at B3LYP/6-31G level. Bond lengths are in angstroms and angles in degrees. The structure labels refer to the description in the main text.

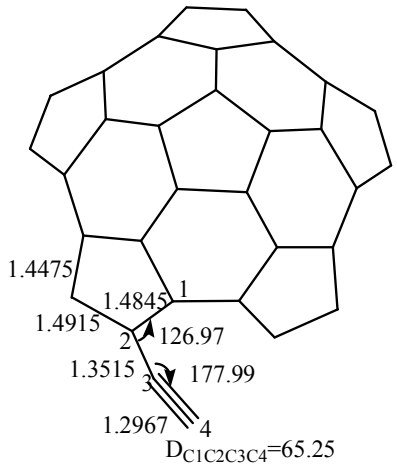

^{1}Cap55-C_2

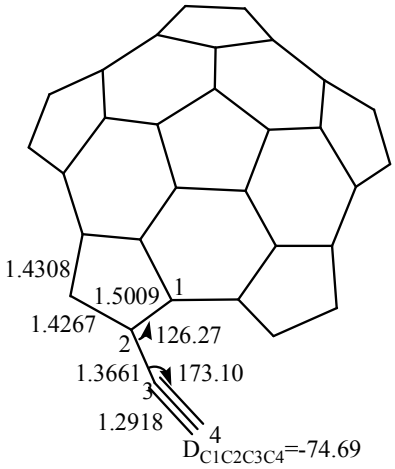

^{3}Cap55-C_2

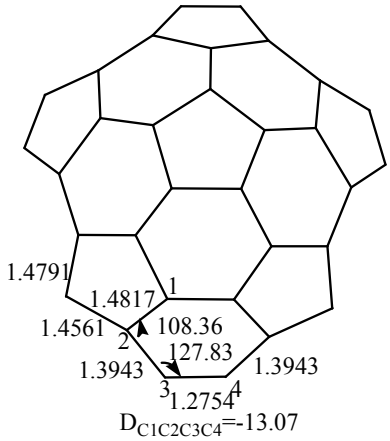

^{1}Cap55+C_2

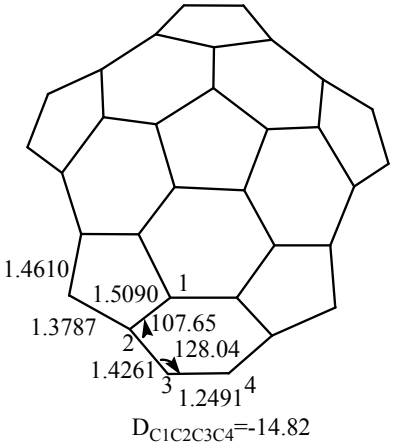

^{3}Cap55+C_2

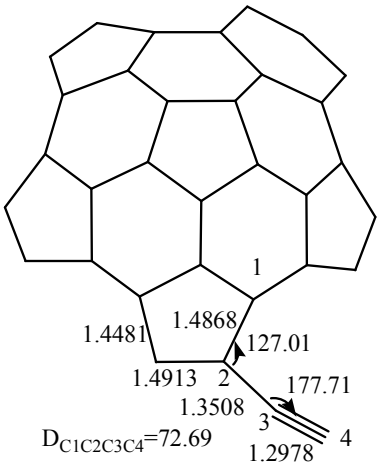

^{1}Int65-C_2

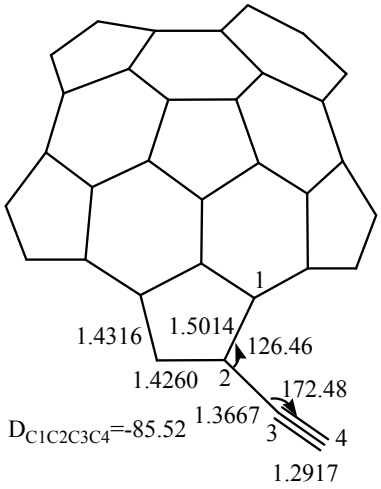

^{3}Int65-C_2

Figure S4 continued

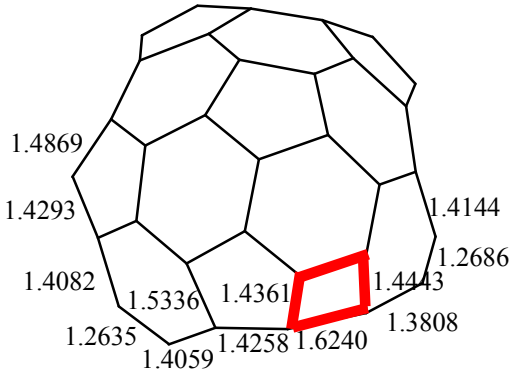

^{1}Int65+C_2

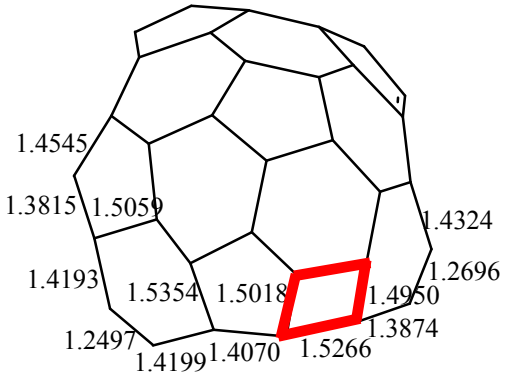

^{3}Int65+C_2

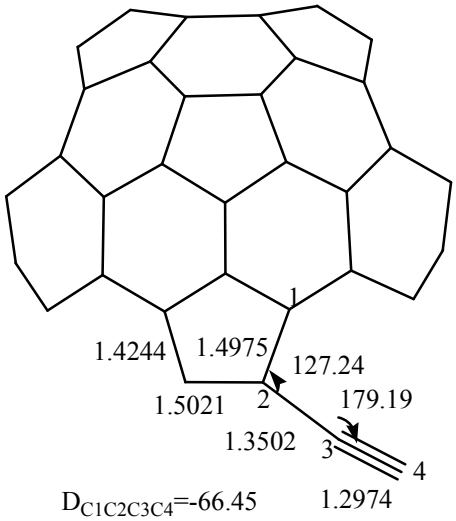

$D_{C1C2C3C4}$=-66.45

^{1}Int75-C_2

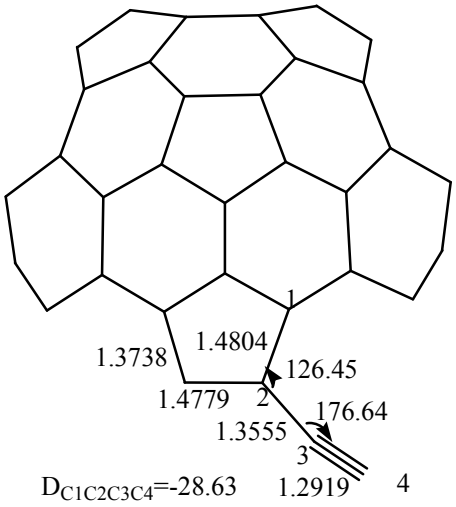

$D_{C1C2C3C4}$=-28.63

^{3}Int75-C_2

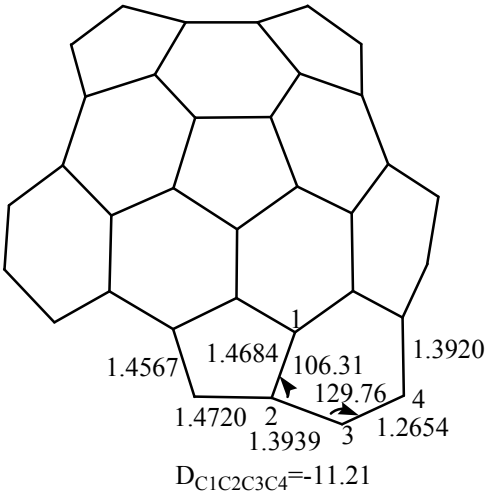

$D_{C1C2C3C4}$=-11.21

^{1}Int75+C_2

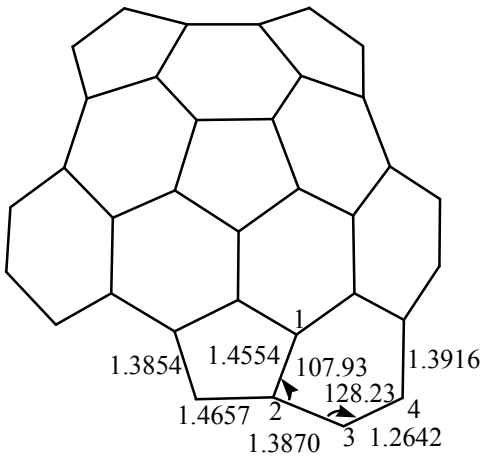

$D_{C1C2C3C4}$=-9.33

^{3}Int75+C_2

Figure S4 continued

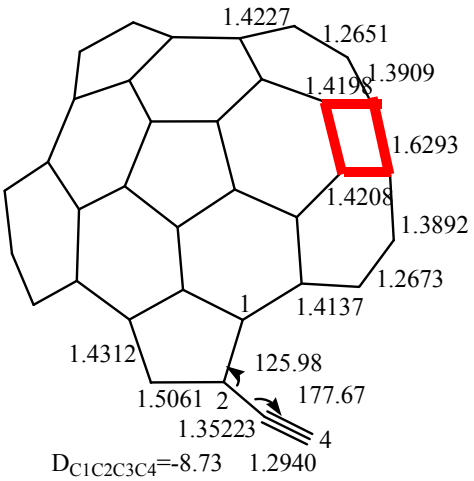

^{1}Int85-C_2

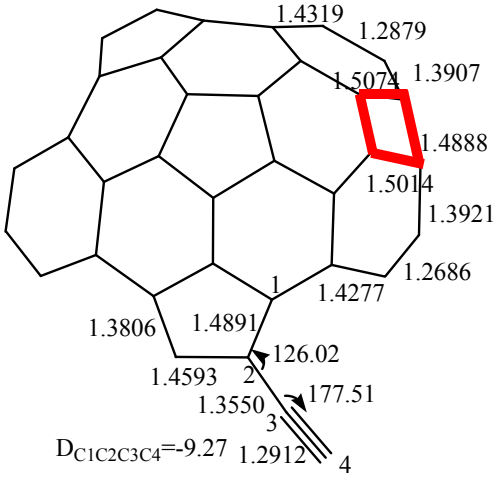

^{3}Int85-C_2

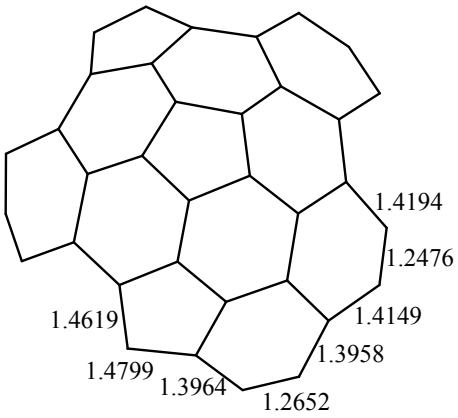

^{1}Int85+C_2

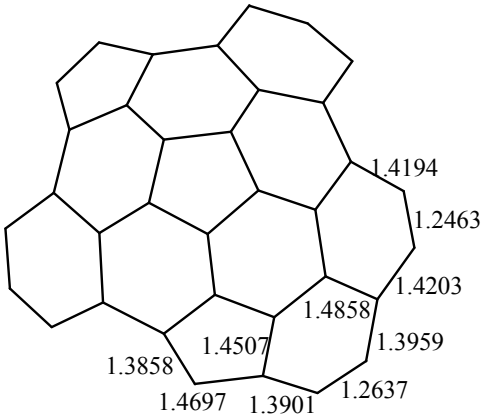

^{3}Int85+C_2

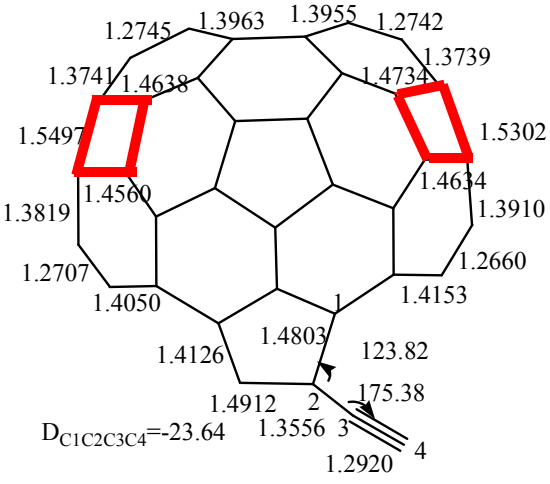

^{1}Int95-C_2

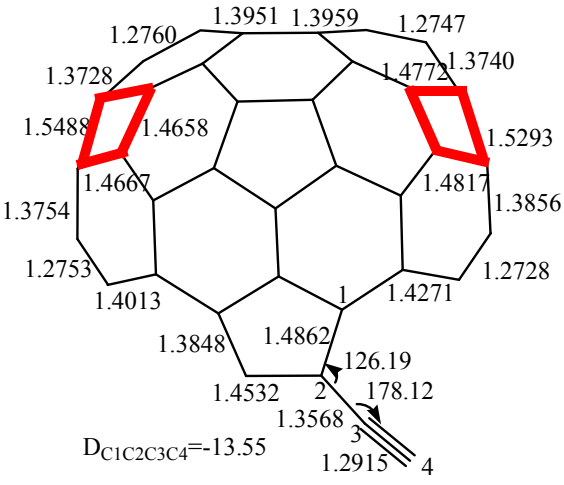

^{3}Int95-C_2

Figure S4 continued

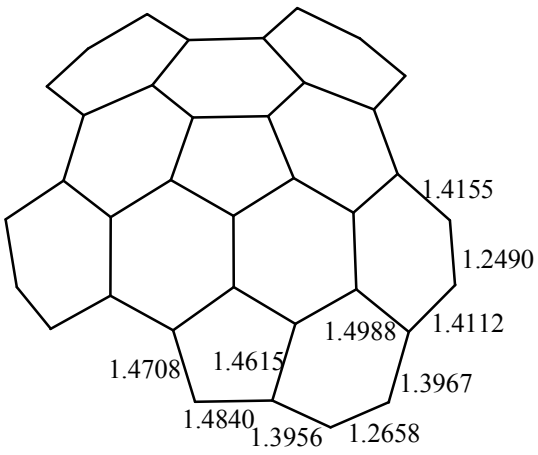

^{1}Int95+C_2

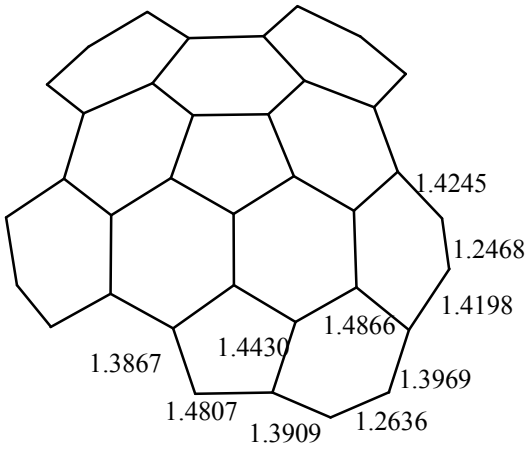

^{3}Int95+C_2

Figure S4 continued

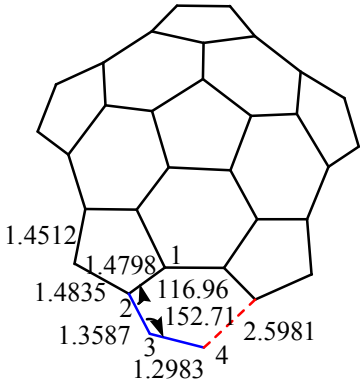

$D_{C1C2C3C4}$=-7.94

^{1}TsCap55-C_2/Cap55+C_2

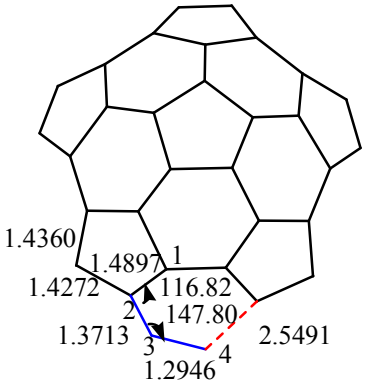

$D_{C1C2C3C4}$=-24.58

^{3}TsCap55-C_2/Cap55+C_2

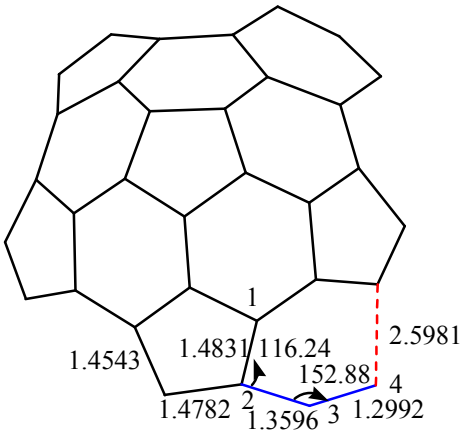

$D_{C1C2C3C4}$=-5.03

^{1}Int65-C_2/Int65+C_2

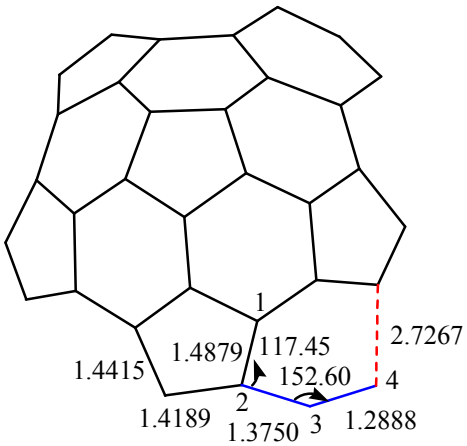

$D_{C1C2C3C4}$=-21.29

^{3}Int65-C_2/Int65+C_2

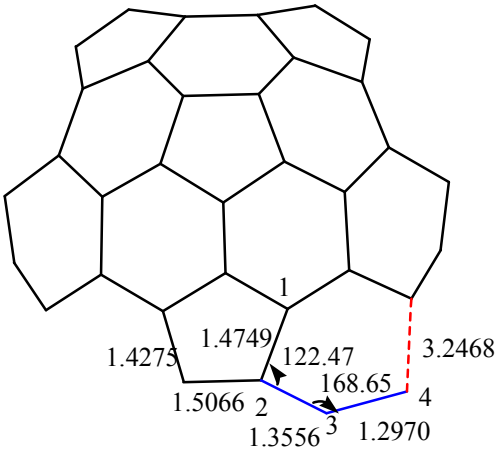

$D_{C1C2C3C4}$=-36.38

^{1}TsInt75-C_2/Int75+C_2

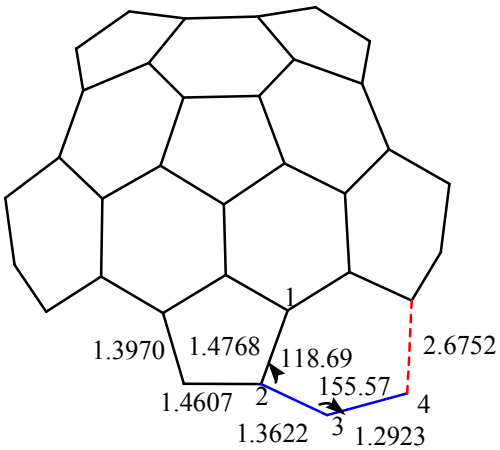

$D_{C1C2C3C4}$=-12.94

^{3}TsInt75-C_2/Int75+C_2

Figure S4 continued

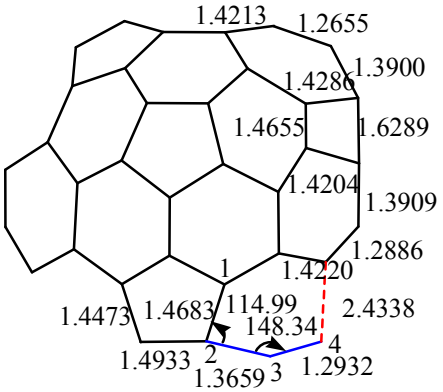

$D_{C1C2C3C4}$=-14.38

^{1}TsInt85-C_2/Int85+C_2

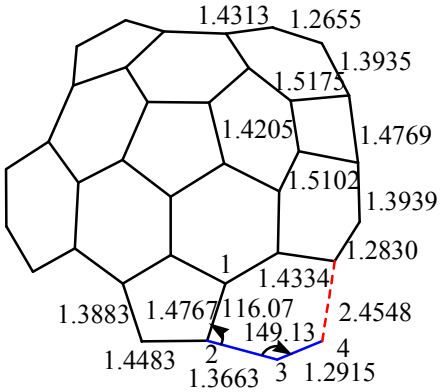

$D_{C1C2C3C4}$=-13.64

^{3}TsInt85-C_2/Int85+C_2

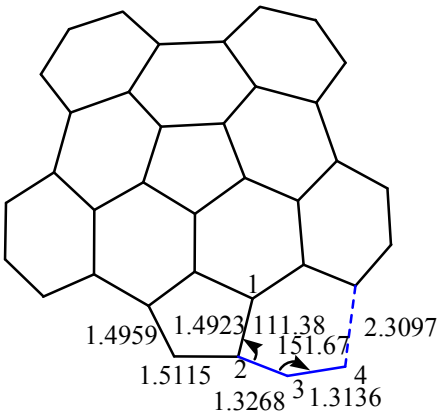

$D_{C1C2C3C4}$=-13.53

^{1}TsInt95-C_2/Int95+C_2

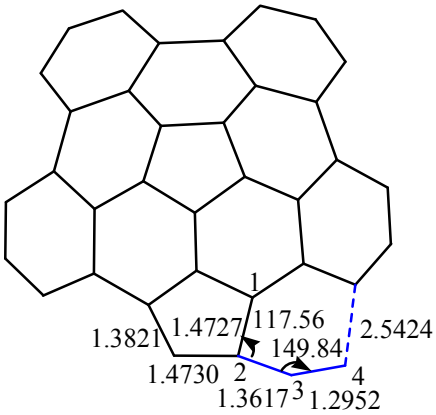

$D_{C1C2C3C4}$=-11.36

^{3}TsInt95-C_2/Int95+C_2